

Impact of land use land cover change on the land surface temperature:

A case study of Shillong

Mebankerlang Nongpiur

PG Diploma in Geoinformatics, Department of Geography, North Eastern Hill University, Shillong, India.

Abstract - Shillong has been experiencing changes in land use land cover over the past years especially in the town areas where a lot of built-ups are emerging. In response to this, there has been some impacts in the distribution of temperature. In this study, remote sensing techniques have been used. The maximum likelihood method has been used for supervised classification of land use land cover from false color composite images. Landsat 5 TM and Landsat 8 OLI/TIRS has been used in this study. The study period is 30 years from 1992 - 2022 with an interval of 15 years. The emergence and increase of more built-up and impervious land cover type surfaces has made the land surface temperature to increase. The correlation between NDVI and LST shows a negative relationship while that of NDBI and LST shows a positive relationship. The temperature has been increasing with an average of 2° C each interval of study. The hotspot analysis has been used to demarcate the heat zones. The highest temperature is found in the crowded and high built-up areas while the lowest temperature is found in the vegetated lands which further cause heat island effect in these highly built-up areas.

Key Words: Land use land cover, Land surface temperature, Change detection, Hotspot analysis, Correlation analysis, Heat-island effect.

1 INTRODUCTION

Changes in LULC have been demonstrated to have a significant impact on the climate which include land surface temperature ([Gogoi et al., 2019](#)). Land surface temperature (LST) is a measurement of the amount of heat emitted from the land surface as a result of various land surface-related activities ([Ramchandra and Kumar, 2009](#)). LST is a crucial physical property of the land surface that is directly controlled by LULC, having consequences for the investigation of climate change and associated environmental effects ([Sobrino & Jiménez-Muñoz, 2014](#)). Only a limited number of studies were undertaken in India by academics, primarily for several major cities like Mumbai, Chennai, Jaipur etc. ([Grover & Singh, 2015](#); [Jalan & Sharma, 2014](#); [Rose Amirtham et al., 2009](#)).

Shillong city has undergone several changes over the years. Due to the area's mountainous and rugged topography, Shillong's land use and land cover had seen tremendous change with development in an unplanned manner ([Ryngnga et al., 2013](#)). The LST of Shillong is also increasing with the changes in LULC. Most of the areas which include the Central Business Districts (CBDs) are undergoing positive changes with emergence and growth of built-up areas and temperature

changes in these areas are also increasing. This has led to the heat island effects. There's a direct relationship between the two where one changes with the change in the other. Limited studies on this relationship have made it an important field of study. Also, the emergence of geo-information technology has added more importance. The analysis of the relationship between urban thermal patterns, spatial structure, and urban surface characteristics using LST, supplemented by thermal infrared bands of remote sensing data from space-borne sensors, is a key use of remote sensing in urban climate studies since it facilitates land use and occupation planning.

Remote sensing and GIS application in this study which include the studies from satellite images especially in the field of climate studies in Shillong is limited. The temperature of Shillong has been increasing owing to the temperature data. Also, distribution of high LST ranges in Shillong is very much clustered to the areas where mostly the commercial and high built-up areas are located.

Several works have been done on LULC relationships and LST and also its impacts particularly in urban areas. ([Neog, 2022](#)) uses the maximum likelihood method was used for LULC classification. NDVI based emissivity approach was used to compute the LST. The LULC has altered, with built-up regions replacing open spaces and vegetation mostly as land is developed. ([Aik et al., 2020](#)) works on the LULC changes and its relationship in LST. The actual temperature and the estimated LST temperature are different. A wider variation of temperature is a result of rising human population, activity levels, and land use. ([Akher & Chattopadhyay, 2017](#)), ([Fatemi & Narangifard, 2019](#)) The NDBI and LST have a positive correlation while the NDVI and LST has a negative correlation. ([Gogoi et al., 2019](#)) temperature rise as result of changes in land use land cover is as significant. ([Halder et al., 2021](#)) indicates heat spots by identifying the highly temperature area.as it is in any developed regions of the world. ([Mehmood & Butt, 2019](#)) as urban areas grow, anthropogenic activities like construction, deforestation, transportation, and infrastructure development increase.

From analysing the related studies, it is found out that most studies used remote sensing data for LULC studies, and are taking urban built-up areas in term of regional as well as global conditions for the LULC-LST relationship. Most of the outcomes of study demonstrates the rise in the built-up area with or from decreasing vegetated land as a result of the greater urbanisation rate which later had resulted to rise in LST in these areas causing heat island effect.

1.1 Aims and Objectives

The aim of the study is to understand and analyse the impacts of land use land cover changes on the land surface temperature of Shillong.

Based on the aim of study, the following objective have been framed.

- i. To detect changes in land use land cover and its impact on land surface temperature.
- ii. To understand and analyse the relationship between land surface temperature and different land use land cover categories using different spectral indices.
- iii. To identify the heat spots/ hotspots of the study and analyse the heat island effect of the city.

1.2 Study Area

Shillong is situated in the eastern part of the state. The city is sizable and extends over a region of land for about 6 kilometers. It is located at an elevation of 1,520 metres (4,990 feet) above sea level. Shillong is an urban agglomeration of Shillong Municipal, Shillong Cantonment and ten other census towns, out of which the Shillong Municipal, Shillong Cantonment and Nongthymmai towns were selected for this study. These three towns have been among the most crowded and busiest or most occupied towns in terms of area in the city

Shillong’s temperature has been increasing. The trend of temperature variation within the years of study is shown in Fig. 1. It can be seen that the mean annual temperature has been on an increasing trend. Similarly, the temperature for the month of March has been increasing as well. This indicates that the temperature in the area has been increasing making the study more relevant. The location map of the study area is shown in Fig. 2.

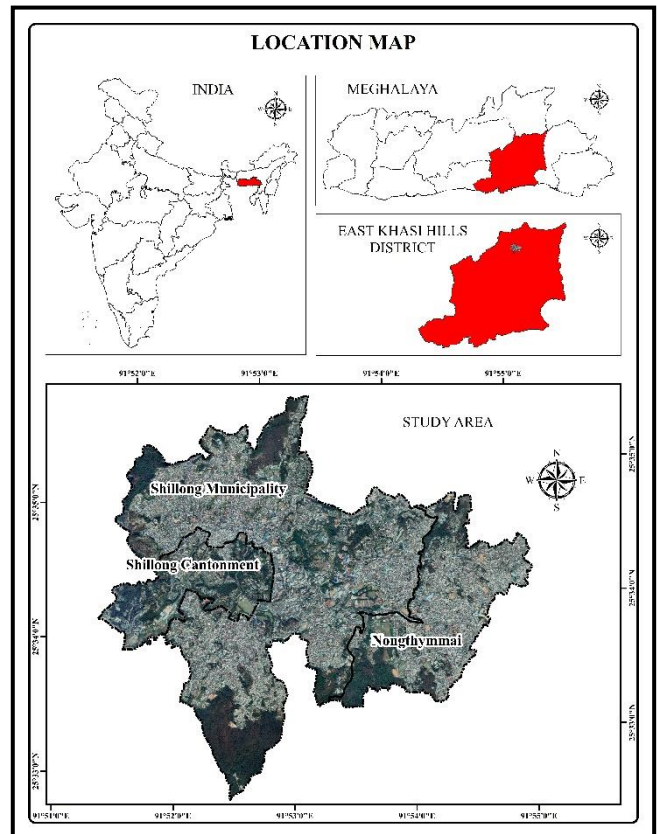


Fig. 2: Location map of study area.

2 DATA AND METHODS

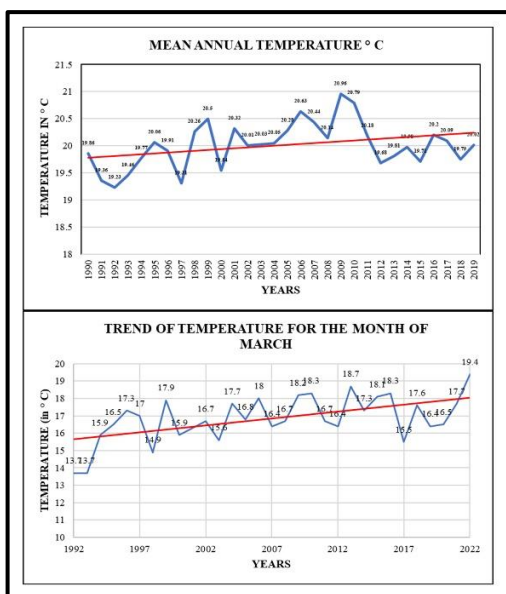
The data/ materials used are Landsat imageries. Level 1 Landsat images were downloaded from USGS Earth Explorer. Three years data been taken in this study with a gap of 15 years. Their details and specifications are mentioned in Table 1. Climatic Research Unit Time Series (CRU TS) v. 4.06 gridded datasets on temperature was used for showing the trend of temperature within study period.

Table 1: Specifications of Remote Sensing data.

Date of Acquisition	Time of Acquisition (GMT)	Datasets	Resolution
26/03/1992	03:41	Landsat 4-5 TM	30 m
20/03/2007	04:12	Landsat 4-5 TM	30 m
13/03/2022	04:17	Landsat 8 OLI/ TIRS	30 m

Table 2: Results of LULC accuracy assessment.

Study Year	Overall accuracy (%)	Kappa Statistics (%)
1992	94.00	87.45
2007	93.00	86.26
2022	90.00	80.56



Source: Climate Research Unit (CRU TS) dataset.

Fig. 1: Trend of temperature of the study area.

Image processing is done using the Arc GIS 10.4 software and ERDAS Imagine 2014. The methods include the supervised maximum likelihood classification for LULC classification.

Table 3: Description of different LULC types taken in the study.

Land cover types	Description
Built-up Area	Built-up areas include those areas covering urban, settlements, residential areas, roads, commercial, educational buildings etc.
Open Land	Open Land include those areas with much of non-vegetated to less significant vegetation cover, impermeable surfaces, bare lands, rock outcrops, open spaces etc.
Water Bodies	Water bodies include all wetlands, ponds, streams, rivers, lakes etc. (Lake is the only feature detected in this study).
Vegetation	Vegetation includes dense as well as sparsely covered vegetated areas ranging from forests, dense bushes, urban green, scrubs, grasses etc.

The single channel algorithm is used for LST estimation. The formula for each step of LST computation are as follows:

2.1 Calculation of top of atmosphere (TOA) radiance

a. For Landsat 5 TM,

$$L\lambda = ((Lmax\lambda - Lmin\lambda) / Qcalmax - Qcalmin) * (Qcal - Qcalmin) - Lmin\lambda \quad (1)$$

where,

- $L\lambda$: TOA Spectral Radiance;
- $Qcal$: Quantized calibrated pixel value in DN;
- $Lmin\lambda$: Spectral Radiance scaled to $Qcalmin$;
- $Lmax\lambda$: Spectral Radiance scaled to $Qcalmax$;
- $Qcalmin$: The minimum Quantized calibrated pixel value in DN;
- $Qcalmax$: The maximum Quantized calibrated pixel value in DN

b. For Landsat 8 OLI/TIRS,

$$L\lambda = M_L * Qcal + A_L \quad (1)$$

where,

- $L\lambda$: TOA Spectral Radiance;
- M_L : Radiance multiplicative scaling factor for the band;
- A_L : Radiance additive scaling factor for the band;
- $Qcal$: Quantized calibrated pixel value in DN.

Secondly, the spectral radiance ($L\lambda$) values are converted to at-satellite Brightness Temperature (TB).

$$TB = \frac{K_2}{Ln\left(\frac{K_1}{L\lambda} + 1\right)} - 273.15 \quad (2)$$

where,

- TB: At-Satellite Brightness Temperature, in Kelvin (K);
- K_1, K_2 : Thermal conversion constants for the band;
- 273.15: Constant for conversion from Kelvin to Celsius.

2.2 Calculation of Normalized Difference Vegetation Index (NDVI)

NDVI is a useful common parameter used for LST studies as it is used for Land Surface Emissivity (LSE) retrieval. In this study, NDVI is used to show the correlation between LST and NDVI.

NDVI is computed using the formula:

$$NDVI = \frac{NIR-Red}{NIR+Red} \quad (3)$$

where,

NIR is the near-infrared spectral band and Red is the red spectral band.

Values of NDVI are range between -1 and +1, where values close to -1 indicate low and sparse vegetation, and values close to +1 signify dense and healthy vegetation.

a. For Landsat 5,

- NIR= Spectral Band 4
- Red= Spectral Band 3

b. For Landsat 8,

- NIR= Spectral Band 5
- Red= Spectral Band 4

2.3 Calculation of Proportion of Vegetation

Proportion of vegetation or Fractional vegetation is needed for land surface emissivity (LSE). Proportion of vegetation (Pv) is calculated using the formula:

$$Pv = \left[\frac{(NDVI - NDVI_{min})}{(NDVI_{max} - NDVI_{min})} \right]^2 \quad (4)$$

where,

- NDVI: is the NDVI;
- $NDVI_{max}$: is the maximum value of the NDVI range;
- $NDVI_{min}$: is the minimum value of the NDVI range.

2.4 Calculation of Land Surface Emissivity

Land surface emissivity (ϵ) is computed using NDVI and P_v with the formula:

$$\epsilon = 0.004 * P_v + 0.986 \tag{5}$$

where,

- 0.004: is the average emissivity value of bare soil.
- 0.986: is the standard emissivity value for vegetation.

2.5 Calculation of Land Surface Temperature

Lastly, the LST is calculated using details from the parameters calculated. The formula for LST calculation is:

$$LST = \left(\frac{BT}{1 + (0.00115 * 1.4388) * \ln(\epsilon)} \right) \tag{6}$$

For analysing relationships between LULC and LST, different spectral indices were used. These include NDBI and NDVI.

2.6 Calculation of NDBI

Normalized Difference Built-up Index (NDBI) is another popular index for LST studies. NDBI is the index used for built-up area analysis. The calculation formulas for the index depends on different bands and the band numbers are different for Landsat 5 TM and Landsat 8 OLI/TIRS.

- a. For Landsat 5 TM,

$$NDBI = \frac{SWIR - NIR}{SWIR + NIR}$$

where:

- SWIR: Shortwave Infrared Band (Band 5);
- NIR: Near Infrared Band (Band 4);

- b. For Landsat 8 OLI/ TIRS,

$$NDBI = \frac{SWIR - NIR}{SWIR + NIR}$$

where:

- SWIR: Shortwave Infrared Band (Band 6);
- NIR: Near Infrared Band (Band 5);

2.7 Change Detection (CD)

For change detection of the LULC map between different years, the post classification change detection using the union matrix method in ERDAS Imagine software and a transition/change matrix table is prepared in MS Excel.

2.8 Relationship between LST and the indices

The relationships between LST and the different indices can be direct or indirect relationship. For analysing the relationships between LST and the different indices a Scatter plot diagram is created in MS-Excel based on the Pearson correlation coefficient.

2.9 Hotspot analysis for demarcation of heat spots from the LST

The study area is examined and classified into cold and hot spot areas based on Getis Ord G_i^* local statistics model in the ArcGIS software. The separation of these two areas is determined based on a comparison between each feature of LST with its neighboring measure. After comparison, the feature with minimum values is grouped into cold spots while the maximum value is termed into hot spots.

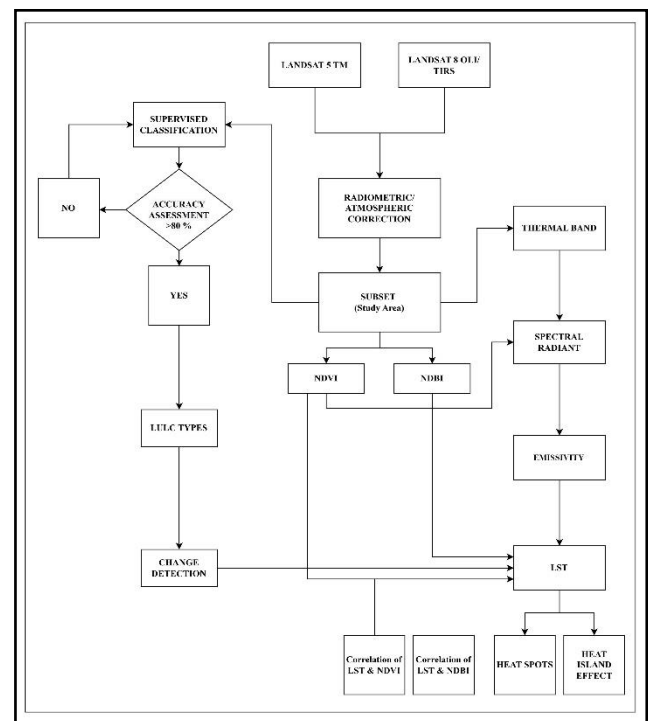


Fig. 3: Methodological Flowchart.

3 RESULTS AND DISCUSSION

Land use/land cover, land surface temperature distribution, LULC change detection, the relationship of LULC and LST, the NDVI, NDBI and their relationships with the LST and the demarcation of heat spot zones of the study area are the primary subsections in which the findings of this study are presented:

3.1 Land use Land cover (LULC)

Land use/ Land cover refers to the data obtained from satellite images that are classified based upon the values of different pixels in an image. These data are generally in the format of raster or grid. Each pixel has a value that links it to a particular class in the classification process. As shown in Table 2, the supervised classification maximum likelihood

was used to create the LULC map in 1992, 2007 and 2022 with high accuracy. The research's overall study area is around 1561.41 hectares. This is the precise region of the LULC categories of this study, as indicated in Table 4 and Fig. 4. The LULC maps show four categories are identified. These categories include built-up areas, vegetation, open land and water bodies. These categories are based on what can be detected from Landsat imageries itself. The LULC maps of 1992, 2007 and 2022 are shown in Fig. 5. The description of the LULC categories is shown in Table 3.

As seen in the results, four classes of the land use land cover are identified. The built-up areas are found to be distributed all across the study area where the more clustered are found in the north-western part of the city considering all the years. This is due to the presence of the central market area and commercial areas which is surrounded by the residential areas. The central part is also seen to have been covered by built-ups in all the three years of study. This is due to the presence of several government offices. The open lands have been decreasing from one period to another. The open lands are found to be distributed in and around the built-up areas. Some of these lands are cleared lands for settlements as well as other infrastructures and the presence of parks, playgrounds etc. which are actually detected to have not much of significant vegetation cover. The vegetation on the other hand is found mostly in the south and extreme north-western part of the study area where community and state forest lands are located. The water body land cover type is however distributed in one place which is a lake area that is in the central part of the city. With time, these land cover types changes. A lot of these changes is further discussed in the change detection section of the study.

Table 4: Area coverage of different LULC types in the study period.

Land cover types	1992		2007		2022	
	Area (Ha)	Area %	Area (Ha)	Area %	Area (Ha)	Area %
Built-up Area	723.52	46.34	890.65	57.04	940.51	60.23
Open Land	311.92	19.98	224.48	14.38	75.82	4.86
Water Bodies	2.16	0.14	2.16	0.14	2.16	0.14
Vegetation	523.81	33.55	444.12	28.44	542.92	34.77
Total	1561.41	100.00	1561.41	100.00	1561.41	100.00

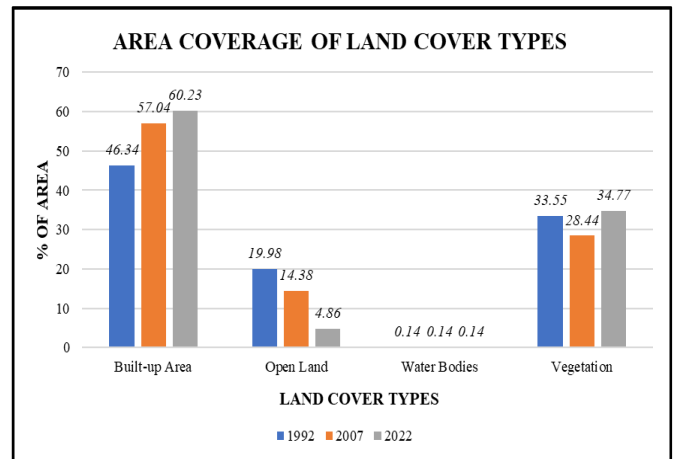


Fig. 4: Area coverage of land cover types.

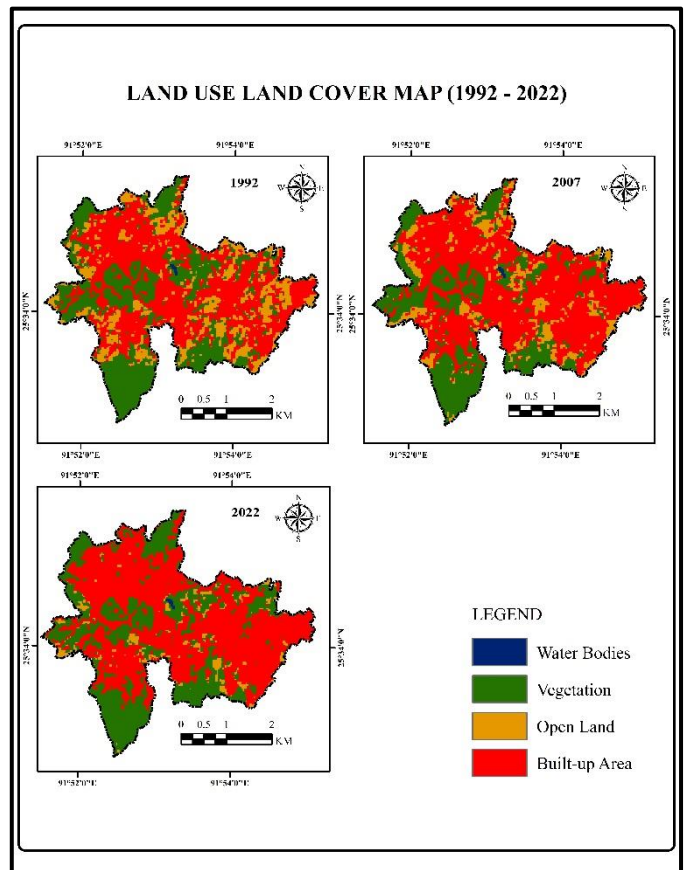


Fig. 5: Land use Land cover maps (1992, 2007 & 2022).

3.2 LULC Change Detection

Different LULC types have transformed over the study period. Some of them change to other land cover types while others remain in the same class with increase in area of coverage. The overall percentage of change in area is shown in

Table 5. The change detection is done using transition matrix of change detection. It identifies each pixel that has change to different land cover types. The table showing the transition matrix of LULC types from 1992 to 2007 and 2007 to 2002 is shown in Table 6 and

Table 7 respectively.

Table 5: Percentage of change in LULC in 1992 – 2022.

Land cover types	% Change (1992 - 2007)	% Change (2007 - 2022)
Built-up Area	10.70	3.19
Open Land	-5.60	-9.52
Water Bodies	0.00	0.00
Vegetation	-5.10	6.33

The LULC types or LULC classes have been changing over the study period. The most changes have been found in the 1992 – 2007 period where about 10.7 % of the area have been added to the built-up area alone in 2007. The high increase of built-up areas especially during the period of 1992-2007 can also be depending on the urban growth of population where more of space is needed for settlements as well as some other developments that occurred where new infrastructures and commercial areas develop. This can be seen in many parts of the Nongthymmai and Laitumkhrach areas located in the eastern part of the city. The transition of open lands to more of the built-up lands in the 2007-2022 period is another change added (3.19 %) to the built-up areas. This can be seen in the north and north western part where most residential areas of Mawprem, Jaiaw Mawkhar and Riatsamthiah. Overall, it's most of the built-up areas that increased converting more of the open lands and vegetated lands to urban built-up areas. Looking at the other classes, open lands shows decrease in by (-)5.60 % and (-) 9.52 % in 1992-2007 and 2007–2022 respectively. Vegetation also decreases in the 1992 – 2007 period with (-) 5.10 % of the areas while it increases in the 2007–2022 period with 6.33 %. The decrease is due to the clearing of significant tree cover converting it to open lands and settlement areas. While in the following period owing to some natural growth of vegetation in the open lands the vegetation increases. However, looking at the water bodies it remains unchanged as the only water body detected is the Wards Lake area. The lake area has not been detected any change as there no expansion or reduction of the lake area while some LULC types around it are changing.

Since the study is conducted using remote sensing data which is satellite images, an advantage of calculating the change/transition matrix which shows changes of each pixel from one LULC type to another. Table 6 and

Table 7 shows the transition matrix of 1992 -2007 and 2007-2022 respectively. It can be detected that there is no change in water bodies from both the tables. As discussed, most changes are seen in the built-up areas where by the different land cover types (except water bodies) are being converted to built-up areas in the study period. The open lands and vegetation are

the other two classes where more area is being added and reduced from one place to another during the course of the study. In Table 6, the built-ups, open lands and vegetation gained area of approximately 57 %, 25% and 17 % respectively. While the loss in area of the classes is approximately 17 %, 47 % and 26% respectively. In

Table 7, the built-up area, open lands and vegetation gained area of approximately 44 %, 11% and 45 % respectively. While the loss in area of the classes is approximately 31 %, 51 % and 18% respectively.

Table 6: LULC change matrix (1992 - 2007)

LULC CLASSES		2007				Grand Total
		Built-up Area	Open Land	Vegetation	Water Bodies	
1992	Built-up Area	661.59	38.61	23.67	0.00	723.87
	Open Land	136.35	139.41	37.53	0.00	313.29
	Vegetation	76.32	56.34	389.43	0.00	522.09
	Water Bodies	0.00	0.00	0.00	2.16	2.16
Grand Total		874.26	234.36	450.63	2.16	1561.41
Gain		212.67	94.95	61.2	0.00	
Loss		62.28	173.88	132.66	0.00	
Net change (ha)		150.39	-78.93	-71.46	0.00	
Net change (%)		17.20	-33.68	-15.86	0.00	

Table 7: LULC change matrix (2007 - 2022)

LULC CLASSES		2022				Grand Total
		Built-up Area	Open Land	Vegetation	Water Bodies	
2007	Built-up Area	769.77	27.45	87.03	0.00	884.25
	Open Land	107.91	42.39	78.21	0.00	228.51
	Vegetation	55.17	11.97	379.35	0.00	446.49
	Water Bodies	0.00	0.00	0.00	2.16	2.16
Grand Total		932.85	81.81	544.59	2.16	1561.41

Gain	163.08	39.42	165.24	0.00	
Loss	114.48	186.12	67.14	0.00	
Net change (ha)	48.6	-146.70	98.10	0.00	
Net change (%)	5.21	-179.32	18.01	0.00	

3.3 Land Surface Temperature Distribution

The land surface temperature refers to the temperature data retrieved from satellite images which is also based on temperature values of different pixels of an image. The single channel algorithm was used for LST retrieval from thermal band 6 and band 10 of Landsat 5 and Landsat 8 respectively. The LST maps is also prepared for all the three years of the study period. The LST maps of 1992, 2007 and 2022 are shown in Fig. 6. The LST ranges is 15° to 27° C, 16° to 29° C and 19° to 30° C for 1992, 2007 and 2022 and the mean LST is approximately 22°, 24° and 26° C respectively. Based on the mean LST, a manual classification method for five classes of LST ranges is prepared for all the years. The area coverage of the LST is shown in Table 8 and Fig. 7.

this rise in the range values. Additionally, climate change may be to blame for these shifts. Based on the classification for all the three years of the study period, the ‘Low’ temperature is distributed mostly towards the southern parts as well as some parts of the north-western part covering the vegetated areas with much of significant tree cover which include parts of the forest areas of Lumparing, Lumpynggad, Risa and Cleve Colony and Lower Mawprem. In 1992 some areas of the Cantonment, the vegetated cover area around the Ward’s Lake area which include the botanical garden shows low temperature. With increase in temperature in the years 2007 and 2022, these areas fall on the ‘moderate’ to ‘high’ temperature ranges. The ‘high’ and ‘very high’ temperature zones covers mostly of the built-up areas which include the settlements, market, commercial as well as other infrastructural areas. The area coverage of the ‘very high’ temperature areas increases owing to the increase of more impervious surfaces around the city. As seen in Table 8, area of the high and very high ranges of temperature increases over the years in the period of study where they cover about 25 % and 59 % of the total area in 2022 respectively. Most of the very high temperature areas is located in mostly the crowded and compacted built-up parts of the city. Since, the study is conducted using remote sensing data, the distribution of temperature may also depend on the time of acquisition of the satellite image. Time is a factor as LST depends on the duration of how the land gets sunlight. Considering the most densely built-up areas which may have been crowded since the earlier periods of the study like the areas of Police Bazar, Iewduh etc. on the north-western portions of the study area, which are market and commercial areas, have always had temperatures higher than the surrounding areas. However, in 1992, only some parts of these areas have temperature higher than 26° C because the time of acquisition of satellite image is approximately 30 minutes earlier at about 9.11 am in the morning. At these times, most of the impervious surfaces are just beginning to heat up depending on the availability of sunlight.

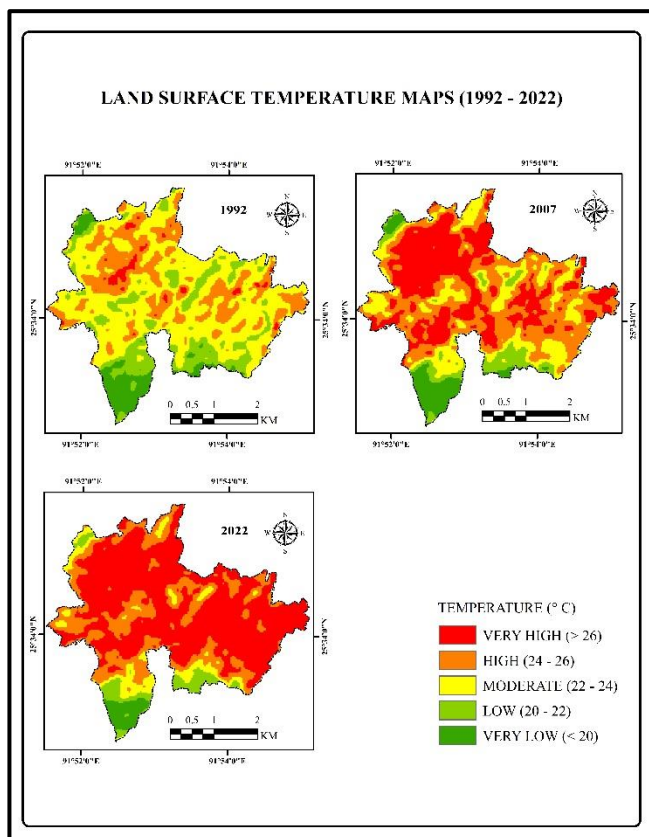


Fig. 6: Land Surface Temperature of the study period (1992, 2007 and 2022).

Table 8: Area coverage of LST ranges in the study period.

LST RANG E (° C)	1992		2007		2022	
	AREA (in Ha)	% AREA	ARE A (in Ha)	% AREA	AREA (in Ha)	%AREA
< 20°	109.89	7.04	97.12	6.22	49.58	3.18
20° - 22°	262.34	16.80	96.21	6.16	75.51	4.84
22° - 24°	773.11	49.51	312.47	20.01	115.45	7.39
24° - 26°	383.04	24.53	549.36	35.18	397.55	25.46
>26°	33.03	2.12	506.25	32.42	923.32	59.13
Total	1561.41	100.00	1561.41	100.00	1561.41	100.00

The LST has been increasing in the 1992-2022 period. The fact that the images were taken at various periods, affecting how the results changed with the seasons, is one reason for

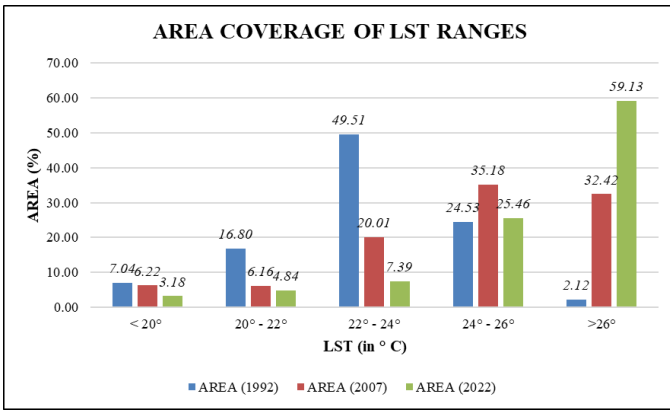


Fig. 7: Area coverage of LST ranges in the study period.

3.4 Relationship between LST and different LULC types

To understand the connection between the LST and different land covers, it is important to study or find out the different thermal signatures of different LULC types. Generally, the LULC classes which shows more of the bare areas and impervious surfaces are detected to have higher temperatures as compared to other LULC types. The mean temperature of each LULC class was computed by averaging all of a given LULC class consistent pixels. The outcome showed that the built-up areas as well as rocky, bare surfaces had the highest LST, while water bodies and the vegetated cover had the lowest. The coldest pixels were found near vegetation and water, while the hottest were found near built-up, impervious surfaces, populated regions, or even barren soil. The pixels' average surface temperature was between 15.50°C and 30.07°C . The differences of mean LST over variations of LULC types is shown in Fig. 8.

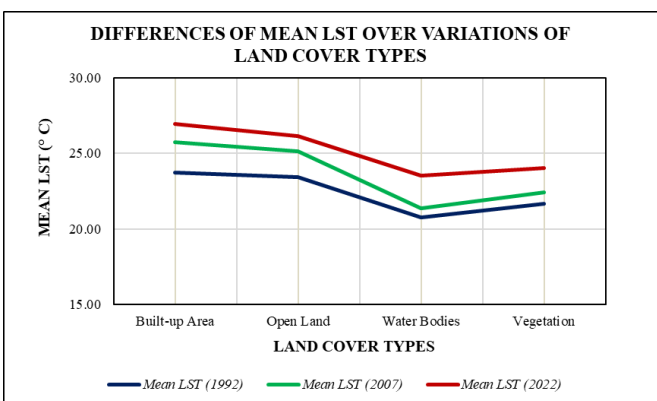


Fig. 8: Differences of mean LST over variations of land cover types.

The characteristics of each LULC types have their own responses to heat source. As mentioned in the results, the more of impervious and built-up surfaces, the higher the LST while the lower the built-ups and higher the vegetation cover the lower is the LST. According to Fig. 8, it can be seen that the built-up areas have higher mean LST followed by open lands, vegetation and water bodies. Water bodies have the lowest mean temperature. This is because water absorbs radiation rather extensively. They also allow for evaporative

cooling. As a result, areas close to water bodies frequently experience milder daytime temperatures. Open lands also show higher LST, this is because most of the Open lands are bare, exposed soil and rock and much of less significant and sparse scrubs and vegetation cover. It can also be found in some areas of the open lands that the temperature is a little higher or equivalent with those on the built-up and concrete areas. This is because the heat from the sun in the vicinity of bare and open lands are absorbed directly into the earth which raises its temperature more quickly than the other LULC types. However, the concrete built-up, pavements, roads, asphalt etc. may absorbs heat slowly, but they tend to have the ability to retain heat longer or releases heat slowly than any LULC types. Looking at vegetation, it is totally different from the built-up and open lands. As discussed, this is because of the tree cover or vegetation cover having the ability to absorb heat and releases it when it gets colder. The outcomes of this study, as to how LST reacts to different land covers agrees with most study where the temperatures will be much higher in the areas of most built-up and concrete surfaces rather than on vegetated lands. Generally, on the overall scale of temperature, it is the built-up areas as well as the vegetation which show high and low temperatures respectively. This relationship can also be shown with the main spectral indices of NDVI and NDBI.

3.5 Relationship between LST and NDVI

The NDVI helps in identification of healthy and dense vegetation cover. To further show LULC alterations' effects on the LST. The NDVI maps are shown in Fig. 10. The ranges of NDVI values are -0.06 to 0.52, -0.18 to 0.59 and -0.14 to 0.65 for the years 1992, 2007 and 2022 respectively. Spectral indices are being calculated and show the relationship with LST. These linkages were examined using the correlation analysis and Pearson's correlation coefficient analysis. The correlation graph between NDVI and LST for all the three years of the study period is shown in Fig. 9.

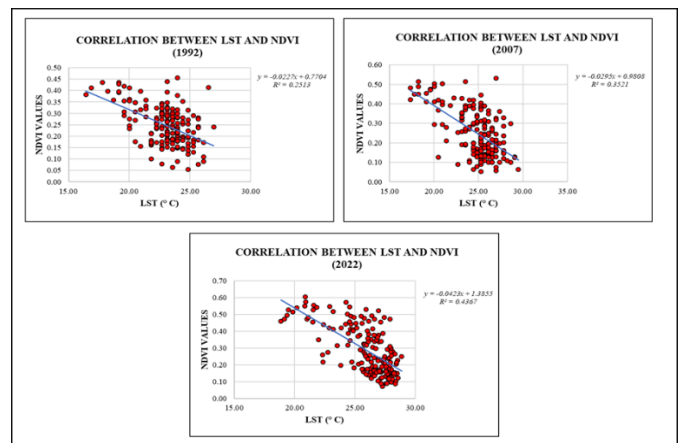


Fig. 9: Correlation of LST and NDVI in the study period (1992, 2007 and 2022).

Fig. 9, shows that LST and NDVI are inversely correlated with one another in all the three years of study. The figure

proves that the LST decrease with increase in NDVI values. The increase in NDVI values shows a greater coverage of vegetation and vice versa. This show, it adheres to the association between the LST and LULC type of vegetation. The first year (1992), shows to have a weak correlation as the dots are more scattered and farther from the trend line with and R^2 value of 0.25 while the years 2007 and 2022 shows a moderate correlation with and R^2 value of 0.35 and 0.5 respectively. Overall, the downward trendline from left to right indicates that there is a weak negative correlation between LST and NDVI.

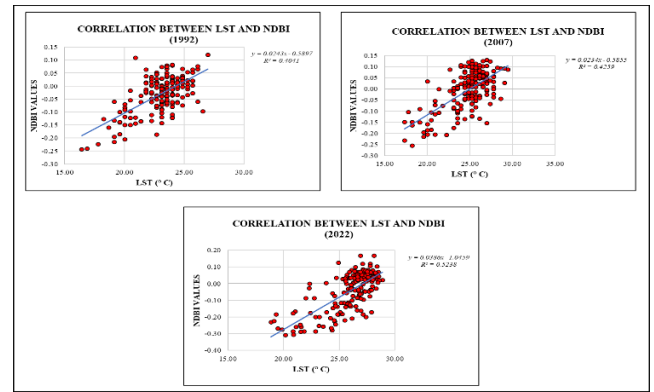


Fig. 11: Correlation of LST and NDBI in the study period (1992, 2007 and 2022).

Fig. 11, shows that there is a positive correlation between the LST and NDBI for all the three years of study. The figure proves that the LST increases with increase in NDBI values. The increase in NDBI values shows a greater coverage of built-up areas and vice versa. This show, it adheres to the relationship between the LST and LULC type of built-up areas. The years of the study period (1992, 2007 and 2022), shows to have a moderate correlation as the dots are more scattered and farther from the trend line with and R^2 value of 0.40, 0.42 and 0.52 respectively. Overall, the upward trendline from left to right indicates that there is a moderate positive correlation between LST and NDBI.

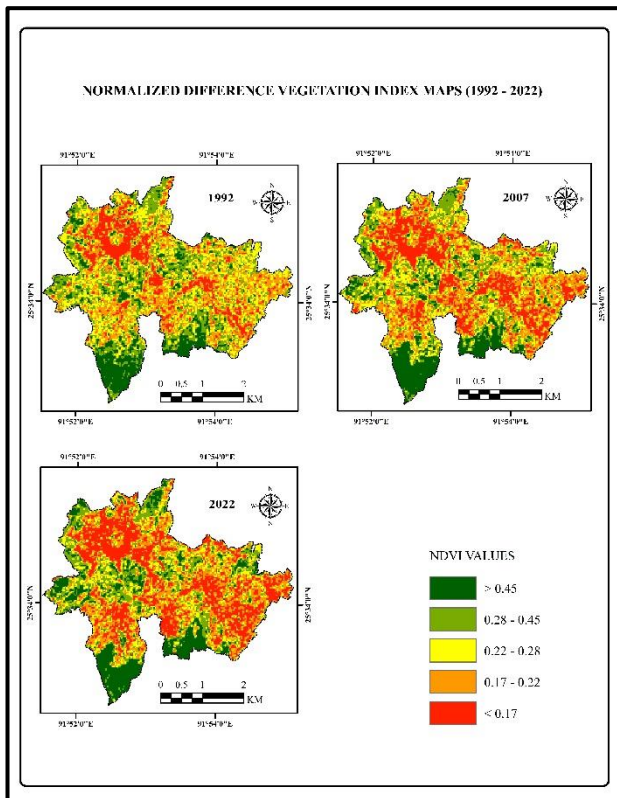


Fig. 10: NDVI maps of the study period (1992, 2007 and 2022).

3.6 Relationship between LST and NDBI

The NDBI helps in identification of built-up areas. The NDBI maps are shown in Fig. 12. The ranges of NDBI values are -0.40 to 0.19, -0.37 to 0.26 and -0.52 to 0.34 for the years 1992, 2007 and 2022 respectively. Here too, the links between the two variables were examined using the correlation analysis and Pearson's correlation coefficient analysis. The correlation graph between NDBI and LST for all the three years of the study period is shown in Fig. 11.

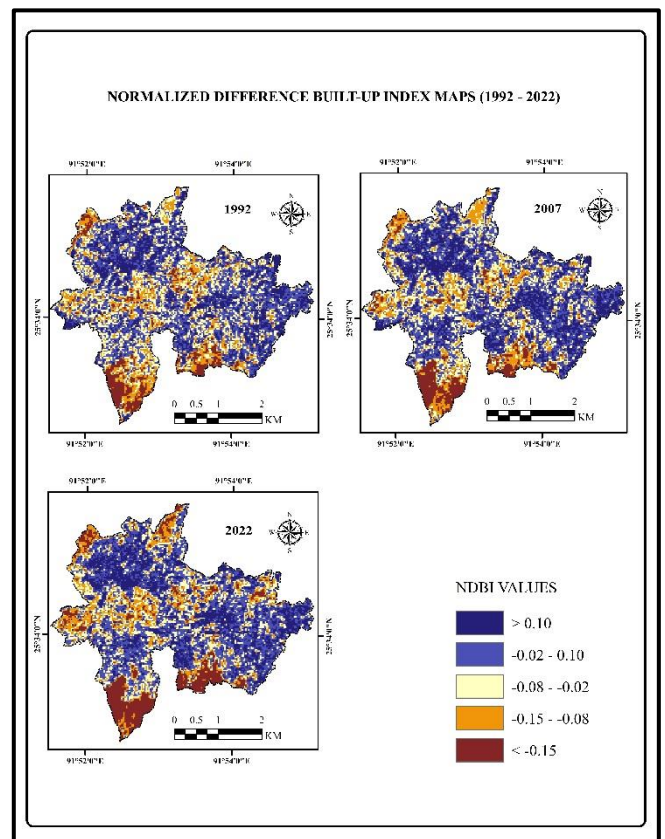


Fig. 12: NDBI maps of the study period (1992, 2007 and 2022).

3.7 Hotspot analysis

Over the study period, the LST of the studied area has increased. This has led to the increase of heat spots or hotspot zones which have relatively higher temperature than the surrounding areas. The hotspot analysis is used to demarcate the hotspot zones. The hotspot analysis maps of the study area are shown in Fig. 13. The overall mean hotspots of the three years of study are also prepared using the cell statistics tool. This is shown in Fig. 14, which shows the overall average hotspots of the area on the mean temperature of the three years.

The changes of LULC areas over the study period has some impact on the LST of the area. These include the increase of LST on the built-up and crowded places. The most heated spots are found mostly on the north-western part of the map. As discussed on the distribution of LST, the most heated spots are found along the densely concrete built-ups, market and commercial areas. Based on the Getis Ord Gi* statistics, the z-score and p-values are taken into consideration which are calculated on the mean LST values of areas of each of the three years of study. Significant hotspots are places with higher z scores and lower p values, whereas significant cold spots are areas with low z scores and low p values. The hotspots zones remain almost the same over the three years as most of the increased built-up surfaces are getting compacted and crowded on the nearby surrounding areas. Some of the land use changes also viz. from open lands to built-up areas especially on the 1992 – 2007 period has shown new emerging hotspots owing to the temperature ranges each year has increased.

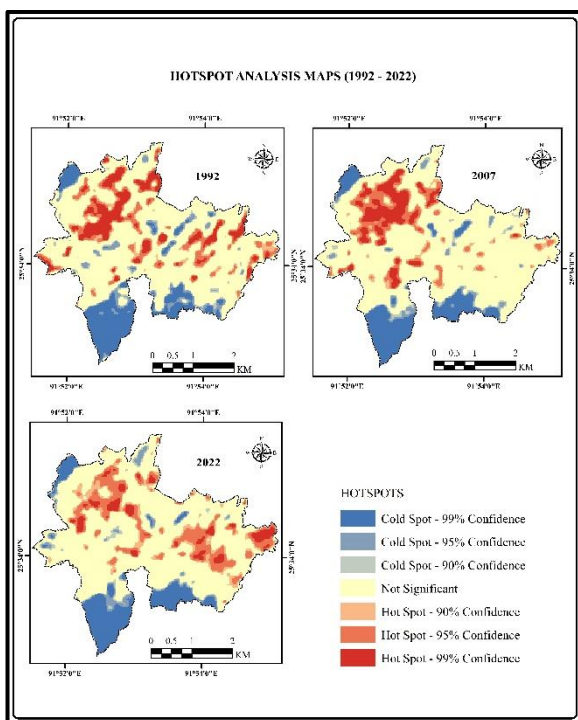


Fig. 13: Hotspot analysis

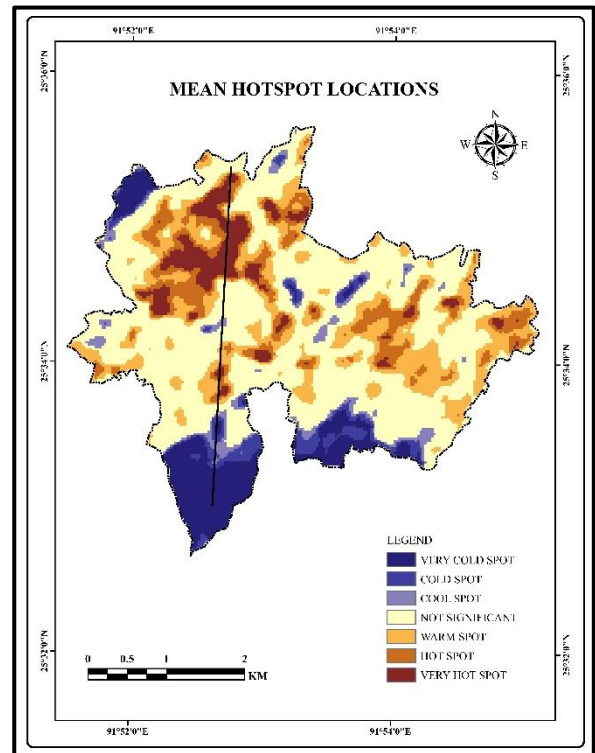


Fig. 14: Mean hotspot zones of the study period (1992, 2007 and 2022).

The overall mean hotspot zones of all the three years of study Fig. 14, shows that the most heated spots still remain the same areas as discussed on the distribution of LST, viz. on the northwest of the study area which include Police Bazaar, Iewduh, Motphran, Mawkhar, Mawprem Jaiaw areas where compacted and congested residences, market and commercial areas are located and also some of the newly emerged hotspots in other parts of the study area including some in the Laitumkhrah and Nongthymmai area. However, the cold spot areas are found on the areas of most vegetated and wooded lands and the rest is the insignificant temperature areas that is they fall in between the hot and cold spots.

3.8 The Heat Island Effect

The heat island effect occurs when land surfaces on an area specifically an urban area, has temperature relatively higher than its surrounding areas, outskirts and vegetated lands. This causes the areas to form some kind of islands of higher temperature, hence the name heat island. In Shillong city, many places are experience change in the temperature with the increasing of concrete built-up surfaces, pavements, road connectivity, walls etc. during the study period. As discussed on the distribution of LST, many areas including the Cantonment area, Central Business District areas including Laitumkhrah, Nongthymmai, Police Bazaar and Iewduh areas are having higher temperatures as compared to other areas with dense vegetated covers including the forested areas of Lumparing and Lumpyngngad areas in the south, the vegetated lands of Lower Mawprem as well as dome other vegetated areas in and around the city.

To show the heat island effect, a profile has been prepared based on a linear distance from north to south covering the different land covers with their LST values. Fig. 14 shows this profile. The profile shows that on a linear distance of approximately 4500 m from north to south, there is a difference in temperature as going through different land covers. It can be seen that the peak of temperature is being covered by the Built-up areas and followed by bare and open lands and vegetation covers. So, it is clear that most of the built-up surfaces around the city are having temperatures higher than the vegetated lands causing the 'Heat-island effect' on the dense built-up surfaces covering most of the highly or more urbanized areas.

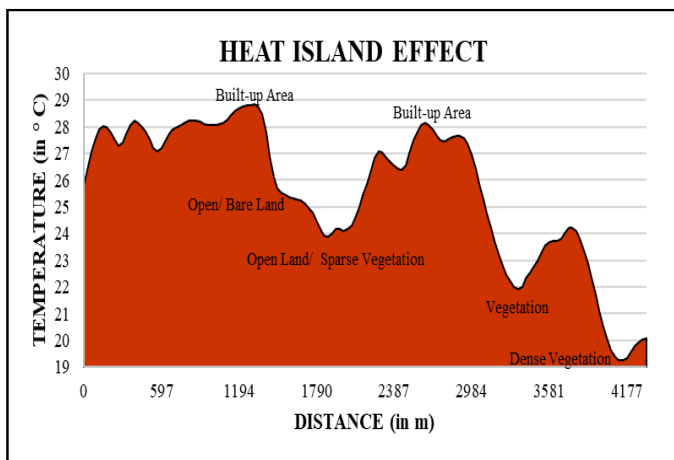


Fig. 14: Heat-island effect

4 CONCLUSION

Through the use of sensing photos downloaded from the USGS website, the variations in LULC and LST are examined in this study to determine if one has an effect on the other. The study period was from 1992 to 2022, a 30-year span, and the data revealed that the built-up areas have grown throughout this time. As a result of these modifications, which is directly related to LST, LST has increased. Effects as observed from the many indices that demonstrate changes in vegetation and built-up areas have a direct and indirect relationship with the increase in LST. Therefore, the increase of LST was influenced by changes in the land use and land cover categories, as well as by an increase in bare and open land.

The analysis of hotspot zones reveals that throughout the entire study period, they increased mainly in the congested, commercial, and highly built-up areas. These changes are a result of the city's increasing impermeable surfaces and concrete built-up areas which can be driven by population and development. The study of LST and hotspot zones for the study period also reveals that it is time dependent where by the LST area coverage is seen to be different in different years of study as a result that satellite images are acquired at different time and duration of when an area receives sunshine.

The limitation of study includes the unavailability of high-resolution data, the requirement of clear skies with least cloud cover for each period of study and the difficulty of analyzing the relationship between LST and air temperature which remains the greatest unknown in remotely sensed studies of heat islands (Nichol et al., 2009). Additionally, climate changes brought on by greenhouse gas emissions are ignored.

Based on the achieved result, it can be recommended that further studies in this field and area should take into consideration other factors that led to temperature increase as well as consider various LULC classes like bare lands and barren lands separately. The relationship of air and surface temperature can also be added.

5 ACKNOWLEDGEMENT

Thanks to the Almighty God for giving me good physical and mental health to complete this paper. My heartfelt gratitude to all the teachers of the Geography Department and PG diploma Geoinformatics course, North Eastern Hill University for their help and ideas shared in related topics to this paper. I would also like to thank my family for their continuous support in my studies. This paper is dedicated to my family.

6 REFERENCES

1. Aik, D. H. J., Ismail, M. H., & Muharam, F. M. (2020). Land use/land cover changes and the relationship with land surface temperature using landsat and modis imageries in Cameron Highlands, Malaysia. *Land*, 9(10), 1–23. <https://doi.org/10.3390/land9100372>
2. Akher, S., & Chattopadhyay, Dr. S. (2017). Impact of Urbanization on Land Surface Temperature - A Case Study of Kolkata New Town. *The International Journal of Engineering and Science*, 6(01), 71–81. <https://doi.org/10.9790/1813-0601027181>
3. Anasuya, B., Swain, D., & Vinoj, V. (2019). Rapid urbanization and associated impacts on land surface temperature changes over Bhubaneswar Urban District, India. *Environmental Monitoring and Assessment*, 191. <https://doi.org/10.1007/s10661-019-7699-2>
4. Atasoy, M. (2020). Assessing the impacts of land-use/land-cover change on the development of urban heat island effects. *Environment, Development and Sustainability*, 22(8), 7547–7557. <https://doi.org/10.1007/s10668-019-00535-w>
5. Fatemi, M., & Narangifard, M. (2019). Monitoring LULC changes and its impact on the LST and NDVI in District 1 of Shiraz City. *Arabian Journal of Geosciences*, 12(4). <https://doi.org/10.1007/s12517-019-4259-6>
6. Gogoi, P. P., Vinoj, V., Swain, D., Roberts, G., Dash, J., & Tripathy, S. (2019). Land use and land cover change effect on surface temperature over Eastern India. *Scientific Reports*, 9(1). <https://doi.org/10.1038/s41598-019-45213-z>
7. Grigoraş, G., & Urişescu, B. (2019). Land Use/Land Cover changes dynamics and their effects on Surface Urban Heat Island in Bucharest, Romania. *International Journal of Applied Earth*

- Observation and Geoinformation, 80, 115–126. <https://doi.org/10.1016/j.jag.2019.03.009>
8. Grover, A., & Singh, R. B. (2015). Analysis of urban heat island (Uhi) in relation to normalized difference vegetation index (ndvi): A comparative study of delhi and mumbai. *Environments - MDPI*, 2(2), 125–138. <https://doi.org/10.3390/environments2020125>
 9. Guite, L. T. S. (2018). Population growth and dynamics of land use/land cover pattern in Shillong urban agglomeration Meghna Basin Land Use Change Analysis and Atlas Development View project Desertification and Land Degradation: Monitoring, Vulnerability Assessment and Combating Plans View project. <https://www.researchgate.net/publication/354780088>
 10. Halder, B., Bandyopadhyay, J., & Banik, P. (2021). Evaluation of the Climate Change Impact on Urban Heat Island Based on Land Surface Temperature and Geospatial Indicators. *International Journal of Environmental Research*, 15(5), 819–835. <https://doi.org/10.1007/s41742-021-00356-8>
 11. Jalan, S., & Sharma, K. (2014). Spatio-temporal assessment of land use/ land cover dynamics and urban heat island of Jaipur city using satellite data. *International Archives of the Photogrammetry, Remote Sensing and Spatial Information Sciences - ISPRS Archives*, XL–8(1), 767–772. <https://doi.org/10.5194/isprsarchives-XL-8-767-2014>
 12. Kaiser, E. A., Rolim, S. B. A., Grondona, A. E. B., Hackmann, C. L., Linn, R. de M., Käfer, P. S., da Rocha, N. S., & Diaz, L. R. (2022). Spatiotemporal Influences of LULC Changes on Land Surface Temperature in Rapid Urbanization Area by Using Landsat-TM and TIRS Images. *Atmosphere*, 13(3). <https://doi.org/10.3390/atmos13030460>
 13. Kikon, N., Singh, P., Singh, S. K., & Vyas, A. (2016). Assessment of urban heat islands (UHI) of Noida City, India using multi-temporal satellite data. *Sustainable Cities and Society*, 22, 19–28. <https://doi.org/10.1016/j.scs.2016.01.005>
 14. Mehmood, R., & Butt, M. A. (2019). Appraisal of Urban Heat Island Detection of Peshawar Using Land Surface Temperature and Its Impacts on Environment. In *Journal of the Indian Society of Remote Sensing* (Vol. 47, Issue 6, pp. 1091–1096). Springer. <https://doi.org/10.1007/s12524-018-0924-6>
 15. Naikoo, M. W., Rihan, M., Ishtiaque, M., & Shahfahad. (2020). Analyses of land use land cover (LULC) change and built-up expansion in the suburb of a metropolitan city: Spatio-temporal analysis of Delhi NCR using landsat datasets. *Journal of Urban Management*, 9(3), 347–359. <https://doi.org/10.1016/j.jum.2020.05.004>
 16. Neog, R. (2022). Monitoring land use dynamics, urban sprawl, and land surface temperature in Dimapur urban area, Nagaland, India. *International Journal of Environmental Science and Technology*. <https://doi.org/10.1007/s13762-022-04378-3>
 17. Nichol, J. E., Fung, W. Y., Lam, K. se, & Wong, M. S. (2009). Urban heat island diagnosis using ASTER satellite images and “in situ” air temperature. *Atmospheric Research*, 94(2), 276–284. <https://doi.org/10.1016/j.atmosres.2009.06.011>
 18. Pal, S., & Ziaul, S. (2017). Detection of land use and land cover change and land surface temperature in English Bazar urban centre. *Egyptian Journal of Remote Sensing and Space Science*, 20(1), 125–145. <https://doi.org/10.1016/j.ejrs.2016.11.003>
 19. Pramanik, S., & Punia, M. (2020). Land use/land cover change and surface urban heat island intensity: source–sink landscape-based study in Delhi, India. *Environment, Development and Sustainability*, 22(8), 7331–7356. <https://doi.org/10.1007/s10668-019-00515-0>
 20. Ramachandra, T. V., & Uttam, K. (2009). Land surface temperature with land cover dynamics: multi-resolution, spatio-temporal data analysis of Greater Bangalore. *International Journal of Geoinformatics*, 5(3), 44.
 21. Rose Amirtham, L., David Devadas, M., Rose, L. A., & Devadas, M. D. (2009). Analysis of land surface temperature and land use/land cover types using remote sensing imagery-a case in chennai city, india. *Architectural design process view project spaash bricks view project analysis of land surface temperature and land use / land cover types using remote sensing imagery-a case in chennai city, india*. <http://glcf.umiacs.umd.edu/index.shtml>.
 22. Rynngga, P., Rynngga, P. K., & L Rynthathiang, B. B. (2013). Dynamics Of Land Use Land Cover For Sustainability: A Case Of Shillong, Meghalaya, India. *international journal of scientific & technology research*, 2. www.ijstr.org
 23. Sobrino, J. A., & Jiménez-Muñoz, J. C. (2014). Minimum configuration of thermal infrared bands for land surface temperature and emissivity estimation in the context of potential future missions. *Remote Sensing of Environment*, 148, 158–167. <https://doi.org/10.1016/j.rse.2014.03.027>
 24. Vorovencii, I. (2014). A multi-temporal Landsat data analysis of land use and land cover changes on the land surface temperature. In *Int. J. Environment and Pollution* (Vol. 56).
 25. Wang, S., Ma, Q., Ding, H., & Liang, H. (2018). Detection of urban expansion and land surface temperature change using multi-temporal landsat images. *Resources, Conservation and Recycling*, 128, 526–534. <https://doi.org/10.1016/j.resconrec.2016.05.011>
 26. <https://www.shillongonline.in/city-guide/geography-of-shillong>
 27. <https://crudata.uea.ac.uk/cru/data/hrg/>